



High Pressure Research

An International Journal

ISSN: 0895-7959 (Print) 1477-2299 (Online) Journal homepage: <http://www.tandfonline.com/loi/ghpr20>

Pressure-induced polyamorphism in $\text{Nd}_{60}\text{Fe}_{30}\text{Al}_{10}$ and $\text{Ce}_{70}\text{Al}_{10}\text{Cu}_{20}$ metallic glasses by high-energy X-ray diffraction and electrical resistance measurements

HPSTAR
495-2017

Linji Zhang, Junlong Wang, Fei Tang, HongWang Yang, Xiuru Liu, Yong Zhao & Wenge Yang

To cite this article: Linji Zhang, Junlong Wang, Fei Tang, HongWang Yang, Xiuru Liu, Yong Zhao & Wenge Yang (2017) Pressure-induced polyamorphism in $\text{Nd}_{60}\text{Fe}_{30}\text{Al}_{10}$ and $\text{Ce}_{70}\text{Al}_{10}\text{Cu}_{20}$ metallic glasses by high-energy X-ray diffraction and electrical resistance measurements, High Pressure Research, 37:1, 11-17, DOI: [10.1080/08957959.2016.1269898](https://doi.org/10.1080/08957959.2016.1269898)

To link to this article: <http://dx.doi.org/10.1080/08957959.2016.1269898>



Published online: 08 Jan 2017.



Submit your article to this journal



Article views: 17



View related articles



View Crossmark data

Pressure-induced polyamorphism in $\text{Nd}_{60}\text{Fe}_{30}\text{Al}_{10}$ and $\text{Ce}_{70}\text{Al}_{10}\text{Cu}_{20}$ metallic glasses by high-energy X-ray diffraction and electrical resistance measurements

Linji Zhang^{a,b}, Junlong Wang^a, Fei Tang^a, HongWang Yang^c, Xiuru Liu^a, Yong Zhao^a and Wenge Yang^b

^aSchool of Physical Science and Technology, Key Laboratory of Advanced Technologies of Materials, Ministry of Education of China, Southwest Jiaotong University, Chengdu, People's Republic of China; ^bCenter for High Pressure Science and Technology Advanced Research (HPSTAR), Shanghai, People's Republic of China;

^cSchool of Material Science and Engineering, Shenyang University of Technology, Shenyang, People's Republic of China

ABSTRACT

In situ high-energy X-ray diffraction of $\text{Nd}_{60}\text{Fe}_{30}\text{Al}_{10}$ and $\text{Ce}_{70}\text{Al}_{10}\text{Cu}_{20}$ metallic glasses is carried out under high pressure. During compression, $\text{Ce}_{70}\text{Al}_{10}\text{Cu}_{20}$ and $\text{Nd}_{60}\text{Fe}_{30}\text{Al}_{10}$ exhibit a polyamorphic transition from low-density state below 2.0 and 10.0 GPa, to high-density state above 8.4 and 21.1 GPa, respectively. The intermediate hysteresis regions are the mixture of both phases. Electrical resistance measurements under high pressure show that $\text{Ce}_{70}\text{Al}_{10}\text{Cu}_{20}$ display a discontinuous change in pressure dependence curve of resistivity at around 1.7 GPa. The addition of Fe atom gives a significant standoff of phase transition pressure in $\text{Nd}_{60}\text{Fe}_{30}\text{Al}_{10}$. The results in this work suggest that the solute element and microstructure of lanthanide solvent aggregates have implications on the polyamorphic transition in metallic glasses.

ARTICLE HISTORY

Received 3 June 2016

Accepted 4 December 2016

KEYWORDS

Metallic glasses;
polyamorphism; high
pressure; strip opposite anvil

1. Introduction

Metallic glasses (MGs) have received widespread research interests due to their potential for structural applications. The structural information in MGs can be conjectured from the evolution of the first sharp diffraction peak (FSDP) in high-energy X-ray diffraction pattern [1]. The inverse position of FSDP, $2\pi/Q_1$ (Q is the momentum transfer, $Q = 4\pi\sin \theta/\lambda$, where 2θ is the diffraction angle and λ is the wavelength), provides direct structural information at the atomic level and statistical information of average inter-atomic spacing d according to the Ehrenfest relationship (i.e. $d \propto 1/Q_1$) [2]. The strong correlation between $2\pi/Q_1$ and d has been used to investigate the pressure-induced polyamorphic transition in MGs. Since the polyamorphic transition was firstly observed in $\text{Ce}_{55}\text{Al}_{45}$ MG, a series of lanthanide-based MG such as $\text{Ce}_{75}\text{Al}_{25}$, $\text{Ce}_{70}\text{Al}_{10}\text{Ni}_{10}\text{Cu}_{10}$, $\text{Gd}_{40}\text{Y}_{16}\text{Al}_{24}\text{Co}_{20}$, $\text{Pr}_{60}\text{Cu}_{20}\text{Al}_{10}\text{Ni}_{10}$,

CONTACT Xiuru Liu  xrliu@swjtu.edu.cn  School of Physical Science and Technology, Key Laboratory of Advanced Technologies of Materials, Ministry of Education of China, Southwest Jiaotong University, Chengdu 610031, People's Republic of China; Wenge Yang  yangwg@hpstar.ac.cn  Center for High Pressure Science and Technology Advanced Research (HPSTAR), Shanghai 201203, People's Republic of China

© 2016 Informa UK Limited, trading as Taylor & Francis Group

$\text{Yb}_{60}\text{Ca}_{2.5}\text{Zn}_{20}\text{Mg}_{17.5}\text{Pr}_{75}\text{Al}_{25},(\text{La}_{0.5}\text{Ce}_{0.5})_{64}\text{Al}_{16}\text{Ni}_5\text{Cu}_{15}$ are found to display the discontinuous change of $2\pi/Q_1$ under high pressure, which are attributed to a pressure-induced low-density state (LDS) to high-density state (HDS) transition [3–9]. The transition usually sustains in certain pressure range and the mixture of LDS and HDS phases exist in the intermediate hysteresis regions [3–8]. However, it is essentially difficult to measure an accurate density change to demonstrate the phase transition because the change of volume during transition is very small and the whole sample cannot transform simultaneously under an inhomogeneous pressure environment. Electronic resistance measurement under high pressure is another effective approach to investigate the polyamorphism in MGs. The mechanism of polyamorphism in MGs was frequently ascribed to the lanthanide solvent-component electronic states especially the $4f$ shell [3, 4]. The abrupt change of electronic state of the lanthanide solvent-component and so induced volume change under high pressure could perform as discontinuous electronic resistance change. Liu et al. reported the pressure-induced polyamorphic transition in $\text{Nd}_{60}\text{Al}_{10}\text{Ni}_{10}\text{Cu}_{20}$ by electronic resistance measurement [10], but owing to experiment conditions limit, terminal pressure of phase transition is unavailable. And whether the pressured-induced polyamorphic transition in $\text{Nd}_{60}\text{Al}_{10}\text{Ni}_{10}\text{Cu}_{20}$ could result in discontinuous density change remains unclear. In this work, we study the pressure-induced polyamorphic transition in two typical ternary lanthanide-based MGs $\text{Ce}_{70}\text{Al}_{10}\text{Cu}_{20}$ and $\text{Nd}_{60}\text{Fe}_{30}\text{Al}_{10}$ by combining synchrotron X-ray diffraction and electronic-resistant measurement. Our results provide evidence for the volume collapse during polyamorphic transition in $\text{Nd}_{60}\text{Fe}_{30}\text{Al}_{10}$ and $\text{Ce}_{70}\text{Al}_{10}\text{Cu}_{20}$ MGs by high-energy X-ray diffraction. Electrical resistance measurement provides the coincident transition pressure with X-ray diffraction result for $\text{Ce}_{70}\text{Al}_{10}\text{Cu}_{20}$ MG.

2. Experimental details

$\text{Nd}_{60}\text{Fe}_{30}\text{Al}_{10}$ and $\text{Ce}_{70}\text{Al}_{10}\text{Cu}_{20}$ MGs ribbon was prepared using the single-roller melt spinning. Master ingots were prepared by arc melting a mixture of pure neodymium (99.5 at%), iron (99.2 at%) and aluminium (99.95 at%), and pure cerium (99.5 at%), aluminum (99.95 at%) and copper (99.9 at%) respectively in an argon atmosphere. Amorphous nature of the sample is verified by X-ray diffraction experiments. In situ high-energy X-ray diffraction experiments of $\text{Nd}_{60}\text{Fe}_{30}\text{Al}_{10}$ and $\text{Ce}_{70}\text{Al}_{10}\text{Cu}_{20}$ MGs under pressure are carried out by using symmetrical diamond anvil cell on a 15U1 beamline in the Shanghai Synchrotron Radiation Facility. The amorphous samples were cut into about $80\times92\times32$ and $122\times116\times32 \mu\text{m}^3$ chip and then loaded into a 120 and 150 μm diameter hole of T301 stainless-steel gasket, which was pre-indented to a thickness of about 35 and 40 μm , respectively. Silicone oil was used as the pressure-transmitting media and ruby ball as the pressure calibrate. The wavelength of X-ray was 0.6199 \AA and size of the X-ray spot was $2\times3 \mu\text{m}^2$ (FWHM). The Debye rings were recorded using an image plate in a transmission mode, and the XRD patterns were integrated from the images using the FIT2D software [11]. For calibration of detector to sample distance and detector tilting angles, the diffraction image of a standard CeO_2 was collected for fitting the standard pattern. The background profile was obtained by X-ray through the empty sample chamber without sample and silicon oil only two diamond anvils. Under applied pressure, the MG sample was placed at least 20 min in order to obtain structural stability. The typical time for collecting one set of diffraction patterns was ~ 1 min. Pressure values of before

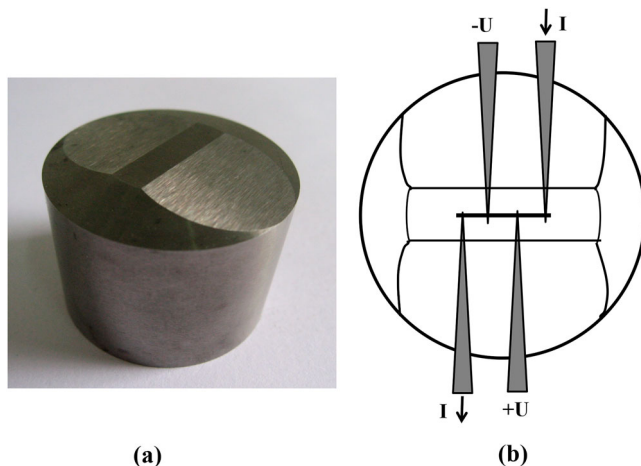


Figure 1. (a) Picture of a strip opposite anvil and (b) schematic diagram of sample assembly.

and after measuring the same spectrum pattern are measured by a well-established Ruby pressure scale. We found that the pressure error was about ± 0.15 GPa.

Electrical resistance measurements under high pressure were carried out in a set-up of strip opposite anvils of tungsten carbide, which is a new type of high pressure mould designed by Hong [12]. Compared with the Bridgman opposite anvil, pressure gradient is small in one-dimensional direction along the central line of the strip opposite anvil. This feature is propitious to the accurate electronic resistance measurement of linear samples under high pressure. The culet size of a strip opposite anvil is 20 mm \times 5 mm and two pieces of 23 mm \times 5.5 mm \times 0.55 mm pyrophyllite were used as gasket. The highest pressure can be up to around 10.0 GPa and details about the strip opposite anvils are described in [12]. Nd₆₀Fe₃₀Al₁₀ and Ce₇₀Al₁₀Cu₂₀ MGs were cut into about 15 mm \times 0.55 mm \times 32 μ m chip and placed on the centre line of the pyrophyllite gasket. Four copper leg wires connect the sample to a constant direct current circuit and an oscillograph was used to record the electrical resistance change under high pressure. The picture of a strip opposite anvil and schematic diagram of sample assembly are shown in Figure 1. The pressure was calibrated by Bi and ZnTe phase transitions.

3. Experimental results

Figure 2(a) and (b) shows selected high pressure X-ray diffraction patterns during compression for the Nd₆₀Fe₃₀Al₁₀ and Ce₇₀Al₁₀Cu₂₀ MGs at room temperature. No sharp Bragg peaks were detected within the studied pressure range, suggesting that the glassy nature of the samples was stable under high pressure at room temperature. Upon compression, the broad diffusive amorphous hole obviously shifts to a higher momentum transfer (Q) due to densification of samples under high pressure. Since the inverse FSDP position $2\pi/Q_1$ correlates with the volume of glass with a power law function [2,13], we use it to estimate the relative volume change under high pressures. The pressure dependence of inverse FSDP position $2\pi/Q_1$ is plotted in Figure 3(a) and (b) for Nd₆₀Fe₃₀Al₁₀ and Ce₇₀Al₁₀Cu₂₀ MGs respectively. In Figure 3(a), the $2\pi/Q_1$ decreases with an increase in pressure and begins to exhibit an obvious deviation from the fitting curve

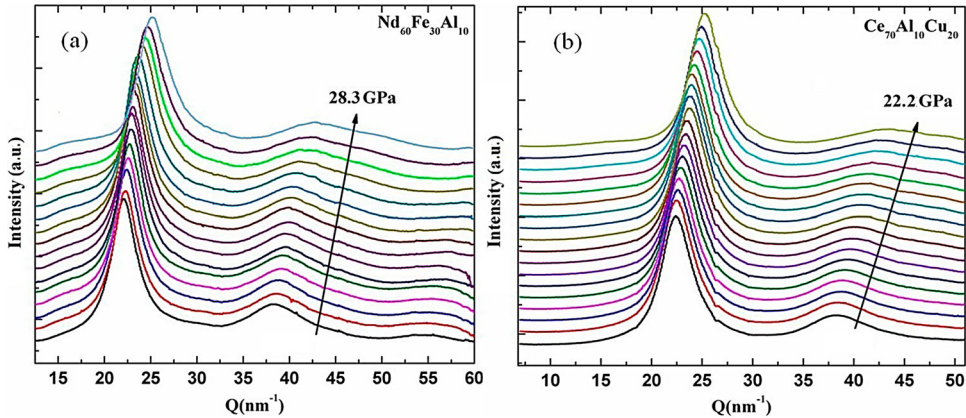


Figure 2. High pressure XRD patterns of $\text{Nd}_{60}\text{Fe}_{30}\text{Al}_{10}$ and $\text{Ce}_{70}\text{Al}_{10}\text{Cu}_{20}$ MGs. Shift of amorphous hole towards higher Q implies the densification of sample under high pressure.

below 10.0 GPa. The deviation proceeds up to 21.1 GPa and then $2\pi/Q_1$ as a function of pressure coincides with a fitting curve above 21.1 GPa. The inverse SDP (second diffraction peak) position $2\pi/Q_2$, which relates to the second neighbour atomic distance, shows similar discontinuous change under high pressure in Figure 3(a). It suggests that there exist two glassy states which are distinctly separated by an intermediate transition region between 10.0 and 21.1 GPa. The anomalous change of $2\pi/Q_1$ for $\text{Nd}_{60}\text{Fe}_{30}\text{Al}_{10}$ MG reveals a polyamorphic transition from LDS to HDS with a volume reduction of about 8.4% (i.e. $2\pi/Q_1 \sim 3.46\%$) at 21.1 GPa. In Figure 3(b), the pressure dependence curve of the inverse FSDP position $2\pi/Q_1$ and inverse SDP position $2\pi/Q_2$ for $\text{Ce}_{70}\text{Al}_{10}\text{Cu}_{20}$ MG also show a discontinuous change over the pressure range of 2.0–8.4 GPa. This observation suggests that $\text{Ce}_{70}\text{Al}_{10}\text{Cu}_{20}$ MG exhibits a polyamorphic transition from an LDS to a HDS with a volume reduction of about 2.7% (i.e. $2\pi/Q_1 \sim 1.1\%$) at 8.4 GPa.

Electronic resistance measurement under high pressure is a complementary approach to investigate the polyamorphism in MGs. The abrupt change of electronic state of the

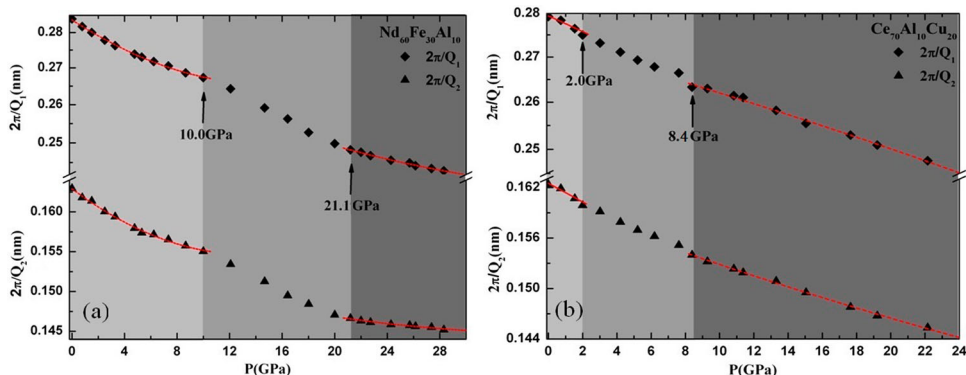


Figure 3. Evolution of inverse FSDP position $2\pi/Q_1$ and reverse SDP position $2\pi/Q_2$ for $\text{Nd}_{60}\text{Fe}_{30}\text{Al}_{10}$ and $\text{Ce}_{70}\text{Al}_{10}\text{Cu}_{20}$ MGs with pressure. Two distinct states with a transition region of about 10.0–21.1 and 2.0–8.4 GPa can be clearly identified for $\text{Nd}_{60}\text{Fe}_{30}\text{Al}_{10}$ and $\text{Ce}_{70}\text{Al}_{10}\text{Cu}_{20}$ MGs respectively.

lanthanide solvent-component and so induced volume change during phase transition could perform as discontinuous electronic resistance change. Pressure-dependent curves of electrical resistivity for $\text{Nd}_{60}\text{Fe}_{30}\text{Al}_{10}$ and $\text{Ce}_{70}\text{Al}_{10}\text{Cu}_{20}$ MGs are illustrated in Figure 4. For $\text{Ce}_{70}\text{Al}_{10}\text{Cu}_{20}$ MG, up on compression the electrical resistance monotonically decreases with increasing pressure. A change of slope is found at around 1.7 GPa. It is due to the result of high-energy X-ray diffraction under high pressure. During the phase transition, the change of electrical resistivity is not sharp and it may be due to the uncompleted phase transition and the mixture of two phases. For $\text{Nd}_{60}\text{Fe}_{30}\text{Al}_{10}$ MG, the electrical resistivity of $\text{Nd}_{60}\text{Fe}_{30}\text{Al}_{10}$ decreases with increasing pressure and there is no discontinuous change within 9.3 GPa.

As mentioned in the introduction part, polyamorphism has been found in series of lanthanide-based MGs. About the mechanism of polyamorphism, the most widespread interpretation is the electronic structural inheritance from the lanthanide solvent elements [3–9]. Lanthanide elements are characterized by a gradual filling of the 4f shell and have a great number of crystal polymorphic transitions for the strongly correlated 4f electrons under high pressure. Liu et al. reported that polyamorphic transitions exist in those lanthanide solvent MGs with 4f electrons by comparing the selected lanthanide-based and non-lanthanide-based MGs [6]. In this work, we found that the non-lanthanide solute elements also have an effect on transition pressure. The phase transition pressure regions in $\text{Ce}_{70}\text{Al}_{10}\text{Ni}_{10}\text{Cu}_{10}$ [5] and $\text{Ce}_{70}\text{Al}_{10}\text{Cu}_{20}$ MGs are 2.0–10.0 and 2.0–8.4 GPa respectively. The phase transition initial pressures $\text{Nd}_{60}\text{Fe}_{30}\text{Al}_{10}$ and $\text{Nd}_{60}\text{Al}_{10}\text{Ni}_{10}\text{Cu}_{20}$ MGs are about 10.0 and 1.2 GPa, respectively [10]. Replacing Cu (10 atom%) by Ni (10 atom%) in $\text{Ce}_{70}\text{Al}_{10}\text{Ni}_{10}\text{Cu}_{10}$ and $\text{Ce}_{70}\text{Al}_{10}\text{Cu}_{20}$ MGs has no obvious impact on the transition pressure. However, replacing Cu (20 atom%) and Ni (10 atom%) by Fe (30 atom%) enhances the transition pressure from 1.2 to 10.0 GPa for $\text{Nd}_{60}\text{Al}_{10}\text{Ni}_{10}\text{Cu}_{20}$ and $\text{Nd}_{60}\text{Fe}_{30}\text{Al}_{10}$ MGs. In addition, $\text{Nd}_{60}\text{Fe}_{30}\text{Al}_{10}$ MG shows exceptional hard magnetic property at room temperature because MGs are usually soft magnetic materials for their non-directional metallic

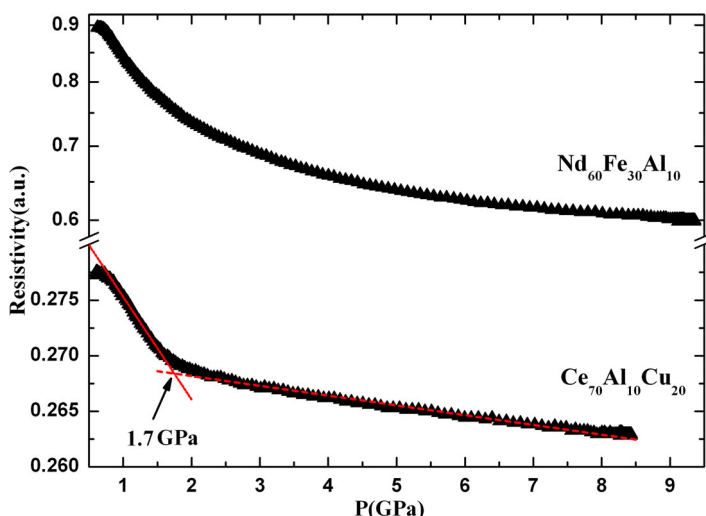


Figure 4. Pressure-dependent curves of electrical resistance for $\text{Nd}_{60}\text{Fe}_{30}\text{Al}_{10}$ and $\text{Ce}_{70}\text{Al}_{10}\text{Cu}_{20}$ MGs.

bonds [14–16]. The mechanism leading to the hard magnetic behaviour of $\text{Nd}_{60}\text{Fe}_{30}\text{Al}_{10}$ MG (and several other Nd-based containing Fe MGs) is still under hot debate [16]. It is presumed to be related to its complex microstructure [15,16]. By using high-resolution scanning electron microscope, it was found that the phase separation during the preparation process of $\text{Nd}_{60}\text{Fe}_{30}\text{Al}_{10}$ MG formed finely dispersed ill-crystallized Nd-rich clusters which embedded in a glassy Fe-rich matrix [15]. In that case, the large elevation in phase transition for $\text{Nd}_{60}\text{Fe}_{30}\text{Al}_{10}$ MG can be properly interpreted by homogeneous deformation hypothesis [17]. These ill-crystallized Nd-rich clusters process a large number of surface atoms. Upon structural transformation, shape deformation of nanoscale Nd-rich clusters results in high-index and high-energy surfaces in the high pressure phase, which destabilizes the high pressure phase and inhibits the phase transition [17]. About the effect of solvent on the transition pressure of lanthanide MGs, Zhao et al. compared the dependence of compressibility on the atom radius of solvent element in $\text{RE}_{55}\text{Al}_{25}\text{Co}_{20}$ ($\text{RE}=\text{Lu, Tm, Er, Ho, Dy, Tb, Pr and La}$) MGs and surmised that the high compressibility of the lanthanide BMGs is related to polyamorphic transition [10]. A larger radius of the larger atoms indicates larger atomic clearance and enables the smaller atoms to enter the clearance more easily [10]. The bulk modulus of $\text{RE}_{55}\text{Al}_{25}\text{Co}_{20}$ MGs is found to decrease with increased atomic radius of solvent element [10]. In this work, the transition pressure of $\text{Ce}_{70}\text{Al}_{10}\text{Ni}_{10}\text{Cu}_{20}$ is slightly higher than that of $\text{Nd}_{60}\text{Al}_{10}\text{Ni}_{10}\text{Cu}_{20}$. It properly indicates that the transition pressure is not related with the atom radius but also the electronic structure of solvent element. Electronic structure hereditary trait of MGs from solvent element or base metal has been discussed intensively [4,6,18]. The results in this work suggest more investigation for the effect of solute element and microstructure of lanthanide solvent element aggregates on the polyamorphism in MGs.

4. Conclusions

The structure of $\text{Nd}_{60}\text{Fe}_{30}\text{Al}_{10}$ and $\text{Ce}_{70}\text{Al}_{10}\text{Cu}_{20}$ MGs under high pressure was studied by *in situ* high-energy X-ray diffraction. The samples exhibited the densification process upon pressure application. During compression, $\text{Ce}_{70}\text{Al}_{10}\text{Cu}_{20}$ and $\text{Nd}_{60}\text{Fe}_{30}\text{Al}_{10}$ MGs show a polyamorphic transition from LDS below 2.0 and 10.0 GPa, to HDS above 8.4 and 21.1 GPa respectively. Electrical resistance measurements show that $\text{Ce}_{70}\text{Al}_{10}\text{Cu}_{20}$ display a change of slope in pressure dependence curve of resistance at around 1.7 GPa. By comparing two sets of Ce-based and Nd-based MGs with same quantity of Ce and Nd solvent elements, we found that the addition of Fe atom gives a significant standoff of phase transition pressure in $\text{Nd}_{60}\text{Fe}_{30}\text{Al}_{10}$. Hereditary traits of MGs from solvent element or base metal were studied intensively. The results in this work may trigger more theoretical and experimental investigation for the effect of solute element and microstructure of lanthanide solvent aggregates on the polyamorphic transition in MGs.

Acknowledgements

We acknowledge the assistance of the staffs of 15U1, Shanghai Synchrotron Radiation Facility (SSRF). We thank S. M. Hong for the assistance in set-up of strip opposite anvils.

Funding

The work was supported by National Science Foundation of China (grant number: U1530402 and 11004163) and Fundamental Research Funds for the Central Universities (grant number: 2682014ZT31), which is supported by Ministry of Education of China.

References

- [1] Ma D, Stoica AD, Wang XL. Power-law scaling and fractal nature of medium-range order in metallic glasses. *Nature Mater.* **2009**;8:30–34.
- [2] Guinier A. X-ray diffraction in crystals, imperfect crystals, and amorphous bodies. New York: Courier Dover Publications; **1994**; p. 61–82.
- [3] Sheng HW, Liu HZ, Cheng YQ, et al. Polyamorphism in a metallic glass. *Nature Mater.* **2007**;6:192–197.
- [4] Zeng QS, Ding Y, Mao WL, et al. Origin of pressure-induced polyamorphism in Ce₇₅Al₂₅ metallic glass. *Phys Rev Lett.* **2010**;104:105702-1-4.
- [5] Duarte MJ, Bruna P, Pineda E, et al. Polyamorphic transitions in Ce-based metallic glasses by synchrotron radiation. *Phys Rev B.* **2011**;84:224116-1-7.
- [6] Li G, Wang YY, Wang PK, et al. Electronic structure inheritance and pressure-induced polyamorphism in Lanthanide-Based metallic glasses. *Phys Rev Lett.* **2012**;109:125501-1-5.
- [7] Zeng QS, Li YC, Feng CM, et al. Anomalous compression behavior in lanthanum/cerium-based metallic glass under high pressure. *Proc Natl Acad Sci.* **2007**;104:13565–13568.
- [8] Lin CL, Ahmad AS, Lou HB, et al. Pressure-induced amorphous-to-amorphous reversible transformation in Pr₇₅Al₂₅. *J Appl Phys.* **2013**;114:213516-1-3.
- [9] Zhao W, Wang YY, Liu RP, et al. High compressibility of rare earth-based bulk metallic glasses. *Appl Phys Lett.* **2013**;102:031903-1-4.
- [10] Liu XR, Hong SM. Evidence for a pressure-induced phase transition of amorphous to amorphous in two lanthanide-based bulk metallic glasses. *Appl Phys Lett.* **2007**;90:251903-1-3.
- [11] Hammersley AP. FIT2D: AN Introduction and overview. ESRF Internal Report 1997; ESRF97HA02T.
- [12] Tang F, Chen LY, Liu XR, et al. A strip anvil apparatus with linear uniform pressure distribution. *Acta Phys Sin.* **2016**;65:100701-1-7.
- [13] Zeng QS, Lin Y, Liu YJ, et al. General 2.5 power law of metallic glasses. *Proc Nat Acad Sci.* **2016**;113:1714–1718.
- [14] Bracchi A, Samwer K, Schneider S, et al. Random anisotropy and domain-wall pinning process in the magnetic properties of rapidly quenched Nd₆₀Fe₃₀Al₁₀. *Appl Phys Lett.* **2003**;82:721–723.
- [15] Schneider S, Bracchi A, Samwer K, et al. Microstructure-controlled magnetic properties of the bulk glass-forming alloy Nd₆₀Fe₃₀Al₁₀. *Appl Phys Lett.* **2002**;80:1750–1751.
- [16] Tan XH, Chan SF, Han K, et al. Combined effects of magnetic interaction and domain wall pinning on the coercivity in a bulk Nd₆₀Fe₃₀Al₁₀ ferromagnet. *Sci Rep.* **2014**;4:6805-1-5.
- [17] Tolbert SH, Herhold AB, Brus LE, et al. Pressure-induced structural transformations in Si nanocrystals: surface and shape effects. *Phys Rev Lett.* **1996**;76:4384–4387.
- [18] Wang WH. Properties inheritance in metallic glasses. *J Appl Phys.* **2012**;111:123519-1-8.